Proceedings of 5th PAAMES and AMEC2012
Dec. 10-12, 2012, Taiwan
Paper No. IR-04

Critical Scenario Prediction of a Bulk Carrier Subjected to Soft Grounding

Yann Quéméner[1], Chien-Hua HUANG[1], Kuan-Chen CHEN[1]
[1] China Corporation Register of Shipping, Taipei, Taiwan

Abstract

This study deals with the ship soft grounding mechanics applied to a Capesize bulk carrier. The ship runs aground by the bow on a smooth seabed. In view of the bow crushing damage, a critical situation is supposed to be met when the collision bulkhead in way of the inner bottom starts being damaged resulting in water ingress in the No.1 cargo hold. Then, for a given ship loading condition and a seabed angle, the critical grounding scenario, characterized by the critical initial forward speed, is assessed. Granted that this speed is exceeded, the critical situation may be reached while the ship rests. First, a mathematical model is proposed to analyze the ship grounding. Then, the mathematical grounding model results are compared to ship grounding dynamic FEAs. Eventually, the mathematical model predictions are found optimistic. Based on the observation of the FEA results, some modifications are identified. Their implementation in a new version of the mathematical model will be the object of a future work.

Keywords: Bow structure, Grounding, Nonlinear FEA

1. Introduction

Statistically, the accidental grounding is a non-negligible risk in ship operation. It is of great concern in regard to the catastrophic consequences that may be expected. Over the past, regulations have been adopted in order to mitigate those consequences in such a way that they would have no immediate impact on the safety of the ship.

For ship bottom tearing and crushing, a double bottom arrangement is provided by the SOLAS (2009) convention, so that the hull split would only affect the double bottom water ballast tank. In a similar way, for soft grounding by the bow (see Fig. 1), the collision bulkhead would limit the water ingress to the fore peak tank and, potentially, to the adjacent double bottom water ballast tank.

The considered ship is a capesize bulk carrier. This study intends to assess the ship critical grounding scenarios as a function of the collision bulkhead location. The grounding scenarios are characterized by the ship critical initial forward speed. Granted that this speed is exceeded, the collision bulkhead in way of the inner bottom is supposed to be damaged while the ship rests.

In the present study, a mathematical grounding model is presented based on the work of Pedersen (1994). This model has for advantage to simplify the grounding mechanics so that the critical initial forward speed can be rapidly evaluated.

This article is divided into four sections. First, the simplified grounding mechanics are presented. In a second part, the bow response to the crushing over the seabed is investigated by FEA. Then, the mathematical grounding model is implemented by combining the nonlinear bow crushing response to the grounding mechanics. Finally, a few time-consuming dynamic grounding FEAs are performed in order to validate the mathematical grounding model.

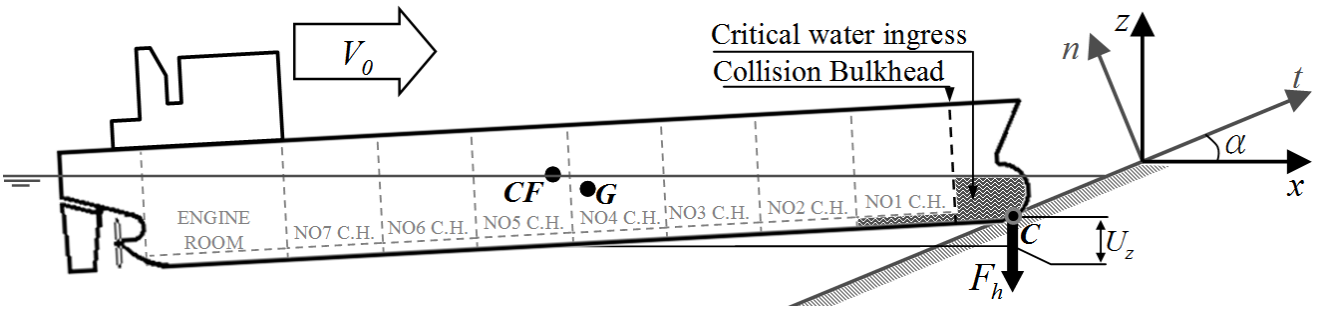

Fig. 1 Ship soft grounding by the bow

2. Grounding mechanics

Pedersen (1994) separated the grounding event into two phases. During those phases, the kinetic energy of the ship is supposed to be dissipated by friction with the seabed, bow structure plastic crushing and increase of the trim. In this study, the seabed is considered rigid so that no energy is dissipated by seabed deformation.

Phase 1: Change in momentum

At the contact between the ship and the seabed, the surge motion of the ship must change to be compatible with the new imposed kinematic restrictions. This is the change in momentum. The ship change of motion is driven by an impulse force, F_I, concentrated in the point of contact C, as presented in Fig. 2.

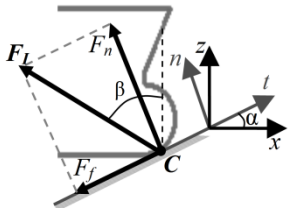

Fig. 2 Impulse force

The impulse direction (β) is determined by considering as valid the Coulomb friction law provided Eq. (1).

$$F_f = \mu \cdot F_n \tag{1}$$

Then, the amount of energy transferred by the impulse force all over the phase 1 is considered equal to the kinetic energy dissipated during phase 1, E_{d1}. To determine the bow velocity v_x, v_y and $\dot{\theta}_y$ in C while the phase 1 ends, Pedersen (1994) established the equations of momentum conservation. The linear momentum conservation perpendicularly to the impulse direction is provided in Eq. (2).

$$V_0 M(1+m_{xx})\cos\beta = v_x M(1+m_{xx})\cos\beta + v_z M(1+m_{zz})\sin\beta \tag{2}$$

where V_0 is the initial forward speed, M the ship displacement. Additionally, m_{xx} and m_{zz} are the added mass coefficients related respectively to the heave and pitch motions.

Then, the angular momentum conservation around the point of contact C is given in Eq. (3).

$$V_0 M(1+m_{xx}) z_G = v_x M(1+m_{xx}) z_G + MR_y^2(1+j_{yy})\dot{\theta}_y + v_z M(1+m_{zz})(x_C - x_G) \tag{3}$$

where x_G and z_G are the coordinate of the center of gravity, R_y is the radius of inertia of mass and j_{yy} is the added mass coefficient related to the pitch motion.

At the end of the phase 1, Pedersen (1994) assumed that the bow would be purely sliding over the seabed. This condition is expressed in Eq. (4).

$$v_z - (x_C - x_G)\dot{\theta}_y = (v_x - z_G\dot{\theta}_y)\tan\alpha \tag{4}$$

From the Eqs. (2), (3) and (4), the bow velocity components in C, as the phase 1 ends, can be determined. As a result, Pedersen expressed E_{d1} as a function of the initial kinetic energy E_0 (see Eq. (5)).

$$E_{d1} = E_0\left[1 - \left(\frac{v_x}{V_0}\right)^2 - a_1\left(\frac{v_z}{V_0}\right)^2 - a_2\left(\frac{R_y\dot{\theta}_y}{V_0}\right)^2\right] \tag{5}$$

where $a_1 = \dfrac{1+m_{zz}}{1+m_{xx}}$ and $a_2 = \dfrac{1+j_{yy}}{1+m_{xx}}$

During the phase 1, the kinetic energy is dissipated by friction with the seabed and bow structure plastic crushing. Here, the grounding mechanics are driven by the bow response to crushing.

Phase 2: Sliding motion

In phase 2, the remaining kinetic energy is dissipated by friction with the seabed, and the trim increase. Here, the grounding mechanics are driven by the trim induced hydrostatic force (F_h) concentrated in C as presented in Fig. 1.

A simplified expression of the trim induced hydrostatic force was proposed by Pedersen (1994) as provided in Eq. (6).

$$F_h = K_h \cdot U_z \tag{6}$$

K_h represents the ship hydrostatic stiffness to the vertical displacement of the center of floatation (CF), induced by the bow lifted distance U_z in C. Its expression is given in Eq. (7).

$$K_h = \frac{\rho \cdot g \cdot A_z}{1 + \left(\frac{x_C - x_{CF}}{R} \right)^2} \tag{7}$$

where A_z is the waterplane area and R is an equivalent radius of inertia expressed in Eq. (8) as a function of the ship mass M and the longitudinal metacentric height (GM_{Long}).

$$R = \sqrt{\frac{M \cdot GM_{Long}}{\rho \cdot A_z}} \tag{8}$$

The phase 2 ends as the initial kinetic energy (E_0) is entirely dissipated.

Scope of the grounding

For the ship herein considered, the energy dissipated in phase 1 (E_{d1}) has been computed from Eq. (5). For seabed angles greater than 30 degrees, E_{d1} is found to be greater than 50% of the initial kinetic energy. Therefore, in this study the grounding is analyzed for angles till 30 degrees. Beyond, it is supposed that the sliding motion characterizing the grounding is significantly reduced.

Then, the bow critical crushing distance ($U_{n,critical}$) is measured till the seabed starts being in contact with the collision bulkhead, as shown in Fig. 3. For this crushing distance, the collision bulkhead in the way of the inner bottom and above is supposed to remain undamaged.

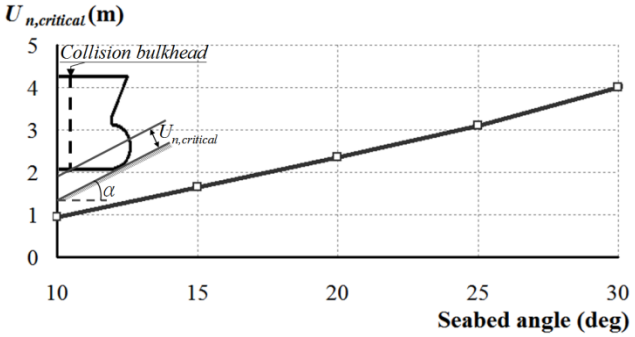

Fig. 3 Critical bow crushing distance

In Fig. 3, it can be observed that the critical crushing is a function of the seabed angle and of the collision bulkhead location. Additionally, as the trim increases during the grounding, the apparent angle between the bow and the seabed decreases, resulting in smaller critical crushing.

3. Bow crushing FEA

Nonlinear explicit Finite Element Analyses (FEA) were carried out in order to extract the response of the bow crushed over the seabed. The FEAs were performed with the explicit dynamic module of ABAQUS.

Bow structure modeling

The extent of the model is longitudinally from the collision bulkhead to the fore end, vertically from the base line to the 3rd panting stringer and transversally from port to starboard. Fig. 4 presents the bow FE model.

Shell elements have been used to mesh the model. The element thickness corresponds to the as-built thickness reduced by half the corrosion margin.

Then, the mesh size has to be fine enough to reproduce the folded configurations of the stiffened panels. A mesh division of 8 elements in the width of typical panels has been chosen, resulting in a global mesh size of 100mm. Eventually, the model contains about 114,000 nodes and 116,000 elements.

Finally, the material properties were defined based on the CR rules (2009). The provided material engineering bilinear stress-strain behaviour was transformed in true stress-strain as for Paik (2007)'s "Material Model I". The stress strain-rate dependency has been expressed following the Cowper-Symonds (1957)' expression.

Boundary conditions

The purpose of those FEAs is to get the bow crushing response related to the seabed angle, independently from the friction, the trim and the crushing velocity effects. Fig. 4 presents the bow crushing modeling.

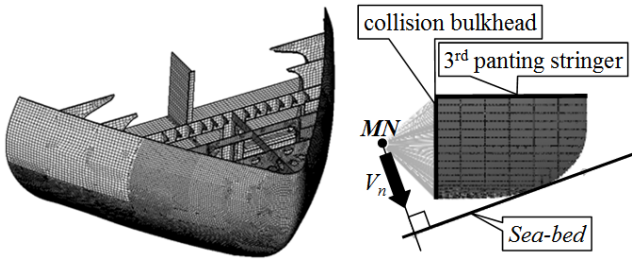

Fig. 4 Bow crushing FE-modeling

The bow is driven by a master node (MN) which couples kinematically all the nodes on the collision bulkhead and the 3rd panting stringer. Therefore, those strong structural members are set up as not deformable.

Then, the crushing FEA are performed without friction and the crushing displacement (U_n) is normal to the seabed rigid surface. Additionally, the ship trim influence on the bow crushing response is neglected.

Finally, since the material behaviour is strain-rate dependent, the crushing velocity (V_n) has a significant influence on the bow crushing response. In order to cover the full range of possible V_n , the crushing FEAs have been carried out for the lowest and highest expected crushing velocities. First, the lowest velocity corresponds to a quasistatic (QS) crushing. The material is taken strain-rate independent and the speed is arbitrarily taken as constant at 5m/s. In quasistatic explicit analyses, artificially increasing the simulation's velocity decreases the time of computation without significant impact on the accuracy of the results. Then, the highest velocity corresponds to a crushing at the ship's maximum forward speed (about 14 knots) on a 45 degrees seabed. This is a conservative case. The V_n is taken as a constant at 5m/s and the material is defined as strain-rate dependent.

Bow crushing response

Fig. 5 presents the bow crushing force (F_n) for a quasistatic crushing and for various seabed angles (α).

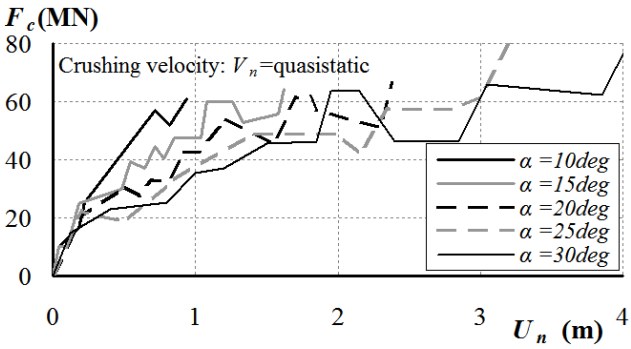

Fig. 5 Bow response to crushing

Plastic strain for critical crushing

Fig. 6 presents the equivalent plastic strain in the bow center-line girder while the critical situation is reached. For that crushing, the 15 degrees seabed is in contact with the collision bulkhead. For more clarity, the plastic strain contour is displayed on the undeformed shape of the structure. Therefore, the area under the seabed surface (dash line) is in fact crushed over the seabed.

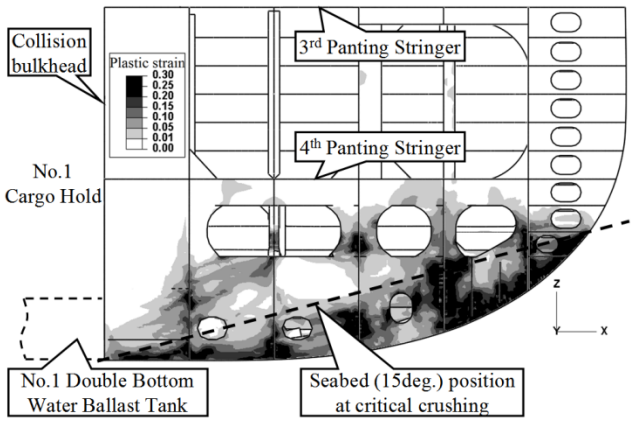

Fig. 6 Plastic strain at critical crushing

In way of the collision bulkhead, from the inner bottom up to the 3rd panting stringer, it can be observed that the plastic strain level is less than 1%. Therefore, no significant deformations are ex-

pected in that part of the collision bulkhead and the No.1 cargo hold is supposed to remain intact.

This low plastic strain state at critical crushing in the vicinity of the No.1 cargo hold has been observed for every investigated FEA of bow crushing over various seabed angles. It can be concluded that the critical crushing distance measurement till the seabed meets the collision bulkhead (see Fig. 3) is valid since the No.1 cargo hold's watertightness is not exposed.

4. Mathematical Grounding Model

The main purpose of the Mathematical Grounding Model (MGM) is to predict the critical initial forward speed $V_{0,critical}$, with an accurate estimate of the final bow crushing. In this section the bow response to crushing (see section 3) is combined to the grounding mechanics (see section 2).

Model implementation

The whole grounding event is driven by a small and constant ship horizontal displacement increment dU_x. At each step i, the bow forces and displacements are evaluated. Then, the total dissipated energy (E_d) is computed as provided in Eq. (9).

$$E_d = \int F_c dU_n + \int F_h dU_z + \int F_f dU_t \qquad (9)$$

The bow response to crushing (F_c) is extracted from the crushing FEAs (see Fig. 5), and the bow crushing displacement (U_n) is computed from the expression given in Eq. (10).

$$U_n(i) = U_n(i-1) + dU_x \sin\alpha \qquad (10)$$

Then, the ship hydrostatic response (F_h) to trim increase is obtained from Eq. (6), and the lifted distance of the bow (U_z) is computed from the expression provided in Eq. (11).

$$U_z(i) = U_z(i-1) + dU_x \tan\alpha \qquad (11)$$

Finally, the friction force (F_f) between the bow and the ground is calculated using the Eq. (1) where the nature of the ground reaction (F_n) depends on the phase. The tangential displacement of the bow over the ground (U_t) is computed from the expression given in Eq. (12).

$$U_t(i) = U_t(i-1) + dU_x \cos\alpha \qquad (12)$$

During phase 1, the ground reaction force F_n is supposed only related to the bow crushing force, while the lift of the bow is neglected (see section 2). Therefore, at each step i, the components in force and displacement $F_c(i)$, $U_n(i)$, $F_f(i)$ and $U_t(i)$ are computed, while F_h and U_z remains to zero. Here, $F_f(i)$ is related to $F_c(i)$ employing the Eq. (1). Then, $E_d(i)$ is calculated and compared to E_{d1}. Granted that $E_d(i)$ is less than E_{d1}, the phase 1 continues.

The phase 2 starts as $E_d(i)$ becomes greater than E_{d1}. Then, during phase 2, at each step i, the components in force and displacement $F_h(i)$, $U_z(i)$, $F_f(i)$ and $U_t(i)$ are computed, while F_c and U_n stagnate. Here, $F_f(i)$ is related to $F_h(i)$ employing the Eq. (1). Then, $E_d(i)$ is calculated and compared to E_0. Granted that $E_d(i)$ is less than E_0, the phase 2 continues.

Critical grounding scenarios

By employing the mathematical grounding model, the ship critical initial speed has been determined in such a way that the critical crushing is reached while the ship rests. Fig. 7 presents the critical grounding scenarios linking the ship critical initial forward speed to the ship loading condition and the seabed angle.

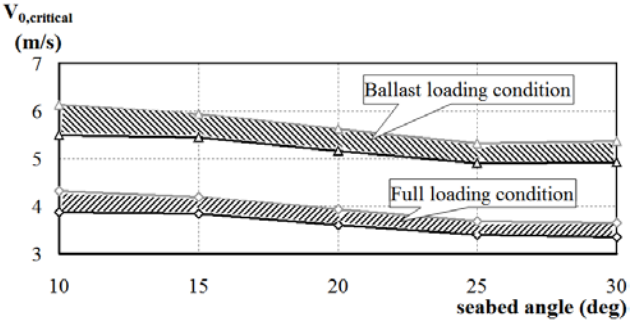

Fig. 7 Critical grounding scenarios

It can be observed that since two crushing velocities (V_n) were defined for the crushing FEAs (see section 3), the predicted $V_{0,critical}$ are comprised between a lower (V_n=*QS*) and upper bound (V_n=*5m/s*). The deviation between the two bounds is only about 10%.

Additionally, the final lifted distance of the bow is found to be less than 5m for the worst cases.

Considering that the grounded ship is in stillwater condition, its yield strength remains sufficient.

5. Ship grounding FEA

In order to validate the accuracy of the MGM predictions, some nonlinear dynamic FEAs are performed (see Fig. 8). The bow FE modeling is the same as previously discussed for the bow crushing FEAs (see section 3). Additionally, the bow interacts with the seabed and with the whole ship.

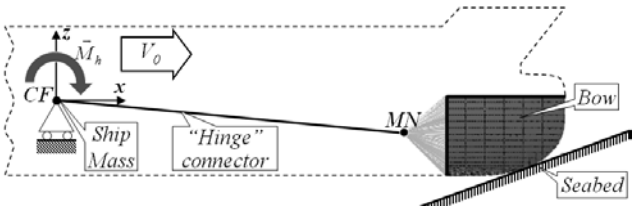

Fig. 8 Ship grounding FE-modeling

Bow/seabed interaction

The friction between the bow and the rigid seabed is defined with a friction coefficient (μ) equal to 0.7.

Bow/ship interaction

During the grounding, the change of trim of the ship is considered small enough to assume that the center of floatation (*CF*, see Fig. 8) remains at the same position. Therefore, to model the pitch and surge motion, the rotation around *Y* and the displacement following *X* are let free in *CF*.

Then, the coupling constraints between the bow and the master node (*MN*) are the same as previously described (see section 3).

A "hinge" connector is modeled between *CF* and *MN*. This hinge allows only one rotation around *Y* at *CF* so that the distance between *CF* and *MN* is constant. Additionally, a linear-elastic moment is included in that hinge at *CF* to model the hydrostatic resisting moment (M_h) which is derived from Eq. (6).

Finally the mass and the inertia of the ship are located in CF. The mass of the ship M_{ship} includes the added mass as provided in Eq. (13).

$$M_{ship} = M\left(1 + m_{xx}\right) \tag{13}$$

The heave and pitch acceleration effects on the grounding mechanics are supposed significant during the phase 1. To ensure the coherence with the MGM assumptions, the heave and pitch acceleration forces have to be carefully considered in the FEA. Based on the previously established momentum conservation in Eqs. (2) and (3), a relation can be derived to link the heave and pitch motions (see Eq. (14)).

$$v_{z(MGM)} = \frac{R_y^2 a_2}{a_1\left[z_G \tan\beta - \left(x_C - x_G\right)\right]}\dot{\theta}_{y(MGM)} \tag{14}$$

However, the FE model imposes a different interrelation (see Fig. 8) as given in Eq. (15)

$$v_{z(FEA)} = \left(x_C - x_{CF}\right)\dot{\theta}_{y(FEA)} \tag{15}$$

To ensure the heave and pitch acceleration forces consistency with the MGM phase 1, the approach herein employed is to scale down the mass moment of inertia around *CF* ($I_{y,CF\ (FEA)}$) as provided in Eq. (16).

$$I_{y,CF(FEA)} = K_{corr} \cdot I_{y,CF} \tag{16}$$

where the correction factor (K_{corr}) is derived from Eqs. (14) and (15), as given in Eq. (17).

$$K_{corr} = \frac{\dfrac{R_y^2 a_2}{a_1\left[z_G \tan\beta - \left(x_C - x_G\right)\right]}}{\left(x_C - x_{CF}\right)} \tag{17}$$

Finally, the heave motion at the center of gravity *G* is considered related to the rotation around *CF*. It has been included into the $I_{y,CF}$ expression as provided in Eq. (18).

$$\begin{aligned} I_{y,CF} &= MR_{y,CF}^2\left(1 + j_{yy}\right) \\ &\quad + M\left(1 + m_{zz}\right)\left(x_G - x_{CF}\right)^2 \end{aligned} \tag{18}$$

Ship grounding scenario

For the MGM validation process, a ship grounding case corresponding to a critical scenario (see Fig. 7) was investigated by FEA. The fully loaded ship is considered running aground on a 20 degrees seabed at an initial velocity of 3.61m/s. The results obtained by FEA have shown that, for this case, the MGM prediction was optimistic. Indeed,

the bow critical crushing has been reached before the ship rests.

Therefore, a second identical FEA has been run for an initial speed reduced by 25% corresponding to 2.71m/s. It was estimated that for this lower speed, the ship will be reaching the critical crushing while it rests. Those FEA results are examined to identify potential improvements relative to the MGM formulation.

MGM comparison to FEA

The MGM formulation, including the criteria identifying the end of each phase, has been established (see sections 2 and 4) according to the evolution of the kinetic energy dissipation, the bow crushing response (F_c) and the ship hydrostatic force (F_h). Therefore, this section focuses on them to compare the MGM to the FEA.

Fig. 9 presents the kinetic energy dissipation evolution over the grounding, assessed by the FEA (thick black line) and the MGM (thin black line). A large deviation appears between the two models. The MGM prediction is significantly more optimistic than the FEA since E_k is dissipated faster.

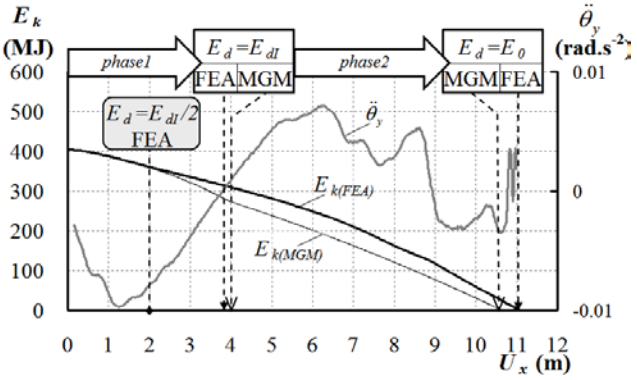

Fig. 9 Kinetic energy dissipation

Then, for $\ddot{\theta}_{y(FEA)}$ (thick grey line) null, the bow motion can be defined as purely sliding over the seabed. Therefore, it corresponds to the end of the phase 1 (E_d=E_{d1}). The MGM and the FEA provide similar ship horizontal displacement (U_x) at that moment of the grounding. Therefore, the coherence discussed earlier (see Eq. (16)) between the two models in phase 1 is confirmed. Additionally, the moment when the ship rests can be identified for each model while E_k becomes null. The span of each phase as well as their respective bounding criteria have been displayed on the top of the figure.

Fig. 10 presents the crushing and hydrostatic force evolution over the grounding assessed by the MGM (thin lines) and the FEA (thick lines). For the FEA, the bow response to crushing is directly derived from the ground normal reaction. Additionally, the hydrostatic force is computed from the hydrostatic moment in *CF*.

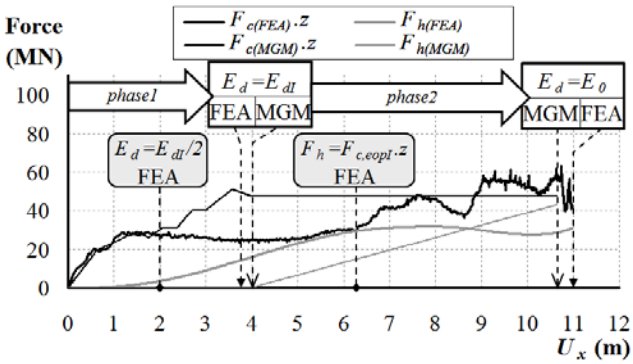

Fig. 10 Evolution of the vertical forces in *C*

First, in phase 1, it appears that the evolution of $F_{c(FEA)}.z$ stops rising before this phase ends. In parallel, $F_{h(FEA)}$ starts increasing. According to the FEA results, a more suitable criterion to end the phase 1 would be to consider half the energy dissipated in phase 1 (E_{d1}) (see Fig. 9). This criterion has been flagged in grey on Figs. 9 and 10.

Then, as the phase 2 starts, the MGM assumed that the grounding mechanics are not anymore governed by the bow crushing response, but by the hydrostatic force (F_h). However, according to the FEA results, the ground reaction ($F_n.z$), equivalent to the bow crushing response ($F_{c(FEA)}.z$), stagnates to the bow crushing response reached at the end of phase 1 ($F_{c,eop1(FEA)}.z$). Therefore, in a new version of the MGM, the friction force should be computed using Eq. (1) where the ground reaction (F_n) is constant and equal to $F_{c,eop1}$.

Finally, the MGM stated that the phase 2 would end while the ship rests. However, before the ship rests, $F_{h(FEA)}$ stops rising, while $F_{c(FEA)}.z$ increases again. This new evolution begins when $F_{h(FEA)}$ reaches $F_{c(FEA)}.z$. Therefore, in a new MGM version, the phase 2 should end at that point and a new third phase should take place. This criterion

has been flagged in grey on Fig. 10. The grounding mechanics of the phase 3 would be identical to the phase 1. The phase 3 would end while the ship rests.

6. Conclusion

In this study, a mathematical model has been proposed to analyze the ship soft grounding mechanics. This model allows for evaluating the critical grounding scenarios characterized by the initial forward speed of the ship. For the fully loaded ship, the critical initial forward speed is comprised between 3.3m/s and 4.3m/s, while for the ballasted condition it is comprised between 4.9m/s and 6.1m/s. This is globally significantly lower than the ship service speed. Additionally, the corresponding maximum lifted distances of the bow are found to remain small enough, so that the hull girder yield strength is not exposed.

Then, the grounding has been investigated by FEA. After comparison, the MGM is found optimistic. Several modifications are identified. They includes new formulations of the phase 1 and 2, and the addition of a final third phase. Their implementation in a new version of the mathematical model will be the object of a future work.

Finally, despite the inaccuracies, the mathematical model has shown it is a practical tool allowing for fast and versatile assessment of the soft grounding mechanics.

List of symbols

English symbols

$a1$, $a2$	Dimensionless ratios for added mass
A_z	Waterplane area
E_0	Initial kinetic energy
E_{d1}	Energy dissipated in phase 1
E_k	Kinetic energy of the ship
F_h	Ship hydrostatic response to trim increase
F_I	Impulse force at contact point
F_c	Bow response to crushing
$F_{c,eop1}$	Bow response to crushing at end of phase 1
F_n	Reaction force normal to the ground
F_t	Frictional force between bow and ground
g	Acceleration of gravity (9.81 m/s^2)
GM_{long}	Longitudinal metacentric height
I_y	Moment of inertia of mass around Y axis
j_{yy}	Added mass coefficient for pitch motion
K_h	Hydrostatic trim resisting stiffness
M	Ship displacement
M_h	Hydrostatic trim resisting moment
m_{xx}	Added mass coefficient for surge motion
m_{zz}	Added mass coefficient for heave motion
R	Equivalent radius of inertia
R_y	Radius of inertia of mass around Y axis
U_n	Bow crushing distance normal to the ground
$U_{n\,critical}$	Critical bow crushing
U_t	Bow sliding distance tangent to the ground
U_x	Longitudinal movement of the bow
U_z	Vertical movement of the bow
V_0	Initial forward speed
$V_{0,critical}$	Critical initial forward speed
V_n	Bow crushing velocity
v_x	Bow surge velocity at the end of phase 1
v_z	Bow heave velocity at the end of phase 1

Greek symbols

α	Seabed angle
β	Impulse force direction angle
$\dot{\theta}_y$	Bow pitch velocity at the end of phase 1
μ	Friction coefficient
ρ	Sea water density

References

China Corporation Register of Shipping 2009 Rules for the construction and the classification of steel ships.

Cowper, G.R. and Symonds, P.S. 1957 Strain-hardening and strain-rate effects in the impact loading of cantilever beams, Technical Report No.28, Division of Applied Mathematics, Brown University, Providence, RI, USA

IMO 2009 The International Convention for the Safety of Life at Sea

Paik, J.K. 2007 Practical techniques for finite element modeling to simulate structural crash-worthiness in ship collisions and grounding (Part I: Theory), SAOS Vol.2, No.1, pp.69-80

Pedersen, P.T. 1994 Ship Grounding and Hull-Girder Strength, Marine Structures, Vol. 7, pp. 1-29.